- Technical Paper -

PREDICTIVE EQUATION FOR SHEAR CARRIED BY STEEL FIBERS IN RC BEAMS BY CONSIDERING STIRRUP RATIO

Pitcha JONGVIVATSAKUL*1, Ken WATANABE*2 and Junichiro NIWA*3

ABSTRACT

The contribution of steel fibers on shear resistance in reinforced concrete with steel fiber (RSF) beams has been studied. Five RSF beams with different stirrup ratio were tested by a four-point bending test. The experimental results indicated that the crack surface displacement and the diagonal crack length of RSF beams decreased with the increase in the stirrup ratio. The shear carried by steel fibers was investigated based on the fracture mechanics. From the experimental results, the empirical equation was suggested to predict the shear carried by steel fibers of RSF beams.

Keywords: reinforced concrete with steel fibers, shear carried by steel fibers, tension softening curve, predictive equation

1. INTRODUCTION

Shear failure in reinforced concrete beams is well-known as brittle behavior. In order to prevent structures from this failure, the JSCE standard specifications have required a large amount of reinforcing bars [1]. This makes it difficult to fill concrete during construction. However, the number of steel bars can be reduced by the application of steel fibers. A great deal of research [2] has reported that the addition of steel fibers improved the shear strength and the ductility of reinforced concrete (RC) members because it helped to resist the formation and growth of crack due to the bridging effect.

JSCE design guidelines for reinforced concrete with steel fibers (RSF) piers [3] have considered steel fibers as the reinforcement of concrete structures. The increment of the shear strength by steel fibers has been expressed as a value κ, which was defined as a ratio of the shear carried by steel fibers to the shear carried by concrete. The equation of RSF for shear capacity proposed in design guidelines recommended the volume fraction of steel fibers in the range between 1.0 and 1.5%, and the value κ was equal to 1.0. However, Watanabe et al. [4] concluded that the values of κ_{exp} were more than 1.0 and varied by the volume fraction of steel fibers (SF) and stirrup ratio (r_w). The combination of steel fibers and stirrups had a synergetic effect to increase the shear capacity of RSF beams. In addition, there was an optimized combination of SF and r_w to increase the value of κ. It was assumed that the optimized combination would be related to the crack surface displacement and the length of the diagonal crack. Nevertheless, there was no verification for the influence of length of the diagonal crack and crack surface displacement on the shear carried by steel fiber of RSF beams.

The objectives of this study were to investigate shear resistance mechanism of RSF beams and develop the equation for calculating the shear carried by steel fibers. This study started with the amount of 1.0% steel fiber in order to demonstrate the hypothesis. In the future, other volume fractions of steel fibers will be used. This paper focused on the tension softening curve, which is one of the fracture mechanics parameters, to evaluate the tensile stress transferring along the diagonal crack. A series of RSF beams with different stirrup ratio were tested. The shear carried by steel fibers was investigated. Finally, the predictive equation for estimating the shear carried by steel fibers was formulated based on the experimental results. The conclusion will be for formulating appropriate design provision for RSF members.

2. TEST PROGRAMS

2.1 Materials

(1) Concrete

The detail of mix proportion is summarized in Table 1. The materials used in the concrete mixes were high-early strength cement, fine aggregates, coarse aggregates and superplasticizer, which was high-performance air entrained (AE) water reducing agent. The concrete was designed with an average 7-day age concrete strength of 50 N/mm^2.

(2) Reinforcements

The longitudinal reinforcing bars used in this research were deformed steel with 25.4 mm nominal diameter. The yield strength was 1016 N/mm^2. The stirrups with deformed steel of 6 mm in diameter were arranged as shear reinforcement. The yield strength was 341 N/mm^2.

(3) Steel fibers

The steel fibers had hooked-end. The aspect ratio

*1 Graduate student, Graduate School of Science and Engineering, Tokyo Institute of Technology, JCI Member
*2 Assistant Prof., Dept. of Civil Engineering, Tokyo Institute of Technology, Ph. D., JCI Member
*3 Prof., Dept. of Civil Engineering, Tokyo Institute of Technology, Dr. E., JCI Member

was 48. The haracteristic of steel fibers are listed in Table 2. The volume fraction of steel fibers to full concrete volume in all specimens was 1.0%.

(4) Specimen fabrication

The test program consisted of five RSF beams with different stirrup ratio. The detail of a tested RSF beam is illustrated in Fig 1. The shear span (a) was 700 mm and effective depth (d) was 250 mm. The shear span to effective depth ratio (a/d) was 2.8. The width of beams was 150 mm.

Two steel bars were arranged as the longitudinal reinforcement of specimens. The longitudinal reinforcement ratio (p_w) was 2.7%. Since this study aimed to investigate the shear carried by steel fibers of RSF beams with different stirrup ratio, the shear reinforcement ratio was varied (i.e. r_w=0.00, 0.12, 0.18, 0.24, and 0.30%). The number of stirrups used in each specimen was changed corresponding to the stirrup ratio. In order to control a side of failure, the number of stirrups in both shear spans was different. The less number of stirrups was provided in the test shear span. For example, in the case of Fig. 1, right side was the test shear span.

Specimens were named according to SF and r_w; e.g. SF10-r12 corresponded to the specimen with SF=1.0% and r_w=0.12%. The name of specimen, r_w and compressive strength (f'_c) of each specimen are summarized in Table 3.

2.2 Loading Method

Specimens were subjected to a four-point bending. The detail is illustrated in Fig. 1. Specimens were placed on the roller supports, which were steel plates with 50 mm width. Teflon sheets and grease were inserted between a specimen and supports in order to prevent the horizontal friction. At loading points, the steel plate with 65 mm width and 150 mm long were also placed.

During the loading test, the applied load was measured. Mid-span deflection was measured using transducers. The strain gauges were used for measuring strain of concrete, longitudinal steel bars at mid-span and strain of stirrups at the middle height.

2.3 Image analysis

The crack surface displacements were calculated by using the displacements of targets obtained from the newly developed system. Higashi et al. [5] have developed the real-time image analyzing system for measuring deformation and strain generated on the surface of specimens.

In order to conduct the image analysis, white color was sprayed on the surface of specimens. Red targets with diameter of 5 mm were attached on the specimen surface with an interval of 20 mm. The purpose of these procedures was to distinguish targets from concrete surface. In order to remove the distortion of images and increase the accuracy of image analysis, the calibration process was conducted before starting the loading test. During the loading test, photos of the specimen were taken by every 5 kN of the shear force

Table 1 Mix proportion of concrete

G_{max} (mm)	W/C	Unit weight (kg/m^3)				
		W	C	S	G	SP
20	0.35	165	471	917	790	5.2

G_{max} = maximum size of coarse aggregate, W = water, C = cement, S = fine aggregate, G = coarse aggregate, SP = high-performance air entrained (AE) water reducing agent

Table 2 Characteristic of steel fiber

Length (mm)	Diameter (mm)	Density (kg/m^3)	Tensile strength (N/mm^2)	Elastic modulus (kN/mm^2)
30	0.62	7850	1050	210

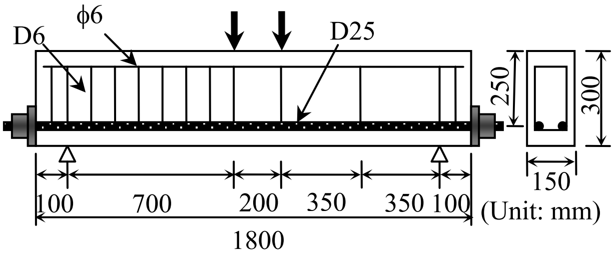

Fig.1 Detail of a RSF beam (SF10-r12)

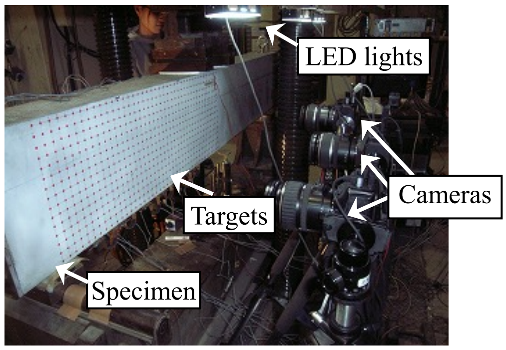

Fig. 2 Loading test

by using three digital cameras fixed on tripods. The white light-emitting diodes (LED) were also used for increasing the accuracy of image analysis. A picture of loading test is shown in Fig. 2. The coordinates of targets were investigated by the image analysis.

2.4 Calculation of the crack surface displacement

Crack surface displacement (u) was defined as the relative displacement of targets on the principal tensile strain direction. The calculation procedure of u is shown in Fig. 3. First, the angle of principal tensile strain (θ) was calculated at the center of square that the crack passed by using Eq. 1. The values of ε_x, ε_y and γ_{xy} in Eq. 1 were measured by image analysis. Then, the relative displacement between two targets that the crack passed (Δx, Δy) (Fig. 3(b)) was calculated using Eq. 2. Finally, crack surface displacement was determined by Eq. 3.

$$\theta = 0.5\tan^{-1}\left\{\gamma_{xy} / \left(\varepsilon_x - \varepsilon_y\right)\right\} \tag{1}$$

$$\Delta x = \Delta x_1 - \Delta x_2, \quad \Delta y = \Delta y_1 - \Delta y_2 \tag{2}$$

$$u = \Delta x \cos\theta + \Delta y \sin\theta \tag{3}$$

where, θ: angle of principal tensile strain, ε_x: strain of x axis, ε_y: strain of y axis, γ_{xy}: the shear strain, (Δx_1, Δx_2): displacement of targets in x direction, (Δy_1, Δy_2): displacement of targets in y direction.

3. EXPERIMENTAL RESULTS AND DISCUSSION

3.1 Calculation method of shear carried by concrete, stirrups, and steel fibers

According to JSCE design guidelines [3], the shear capacity of RSF beams, the shears carried by concrete and stirrups can be calculated as follows:

$$V_{cal} = (1+\kappa)\cdot V_c + V_s \tag{4}$$

$$V_c = 0.2\cdot\sqrt[3]{f_c'}\cdot\sqrt[4]{1000/d}\cdot\sqrt[3]{100p_w}\cdot b_w\cdot d \tag{5}$$

$$V_s = A_w\cdot f_{wy}\cdot(z/s) \tag{6}$$

where, V_{cal}: calculated value of shear capacity of RSF members (kN), κ: coefficient representing the effect of fibers (κ=1.0), V_c: shear carried by concrete (kN), V_s: shear carried by stirrups (kN), f'_c: compressive strength of concrete (N/mm^2), d: effective depth, p_w: longitudinal reinforcement ratio (%), b_w: web thickness (mm), A_w: cross section area of stirrups (mm^2), f_{wy}: yield strength of stirrups (N/mm^2), z: length of moment arm (z = 7d/8) (mm), s: spacing of stirrups (mm).

The experimental value of shear carried by steel fibers ($V_{f\,exp}$) was investigated by Eq. 7. While, the experimental value of κ was calculated by Eq. 8.

$$V_{f\,exp} = V_{exp} - V_c - V_s \tag{7}$$

$$\kappa_{exp} = V_{f\,exp} / V_c \tag{8}$$

where, V_{fexp}: shear carried by steel fibers (kN), V_{exp}: experimental value of shear capacity (kN).

3.2 Shear capacity of RSF beams

Table 3 lists the concrete properties, the details of diagonal crack, the shear force from experiment, the calculated shear carried by steel fibers, and the comparison of experimental values to calculated values of the shear carried by steel fibers. The values of f'_c were from 46.6 to 64.9 N/mm^2. The shear capacity of RSF beams (V_{exp}) was higher than evaluated value and hence all of κ_{exp}: a ratio of $V_{f\,exp}$ to V_c were more than 1.0 as stated in Watanabe et al. [4]. The values of V_{exp} were varied depending on r_w. V_{exp} showed the maximum in SF10-r12 (κ_{exp}=1.57). It is not necessary that the value of V_{exp} in RSF beams will increase with the increase in r_w. This was because of the difference of V_{fexp} in each beam.

3.3 Shear force-deflection of RSF beams

Figure 4 presents the effects of fibers addition and stirrup ratio on the shear force-deflection of RSF beams. The general behavior was similar in all tested beams.

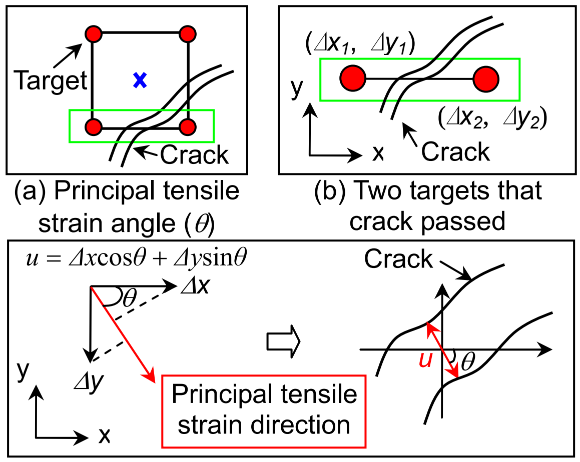

(a) Principal tensile strain angle (θ)

(b) Two targets that crack passed

(c) Crack surface displacement (u)

Fig. 3 Calculating crack surface displacement (u)

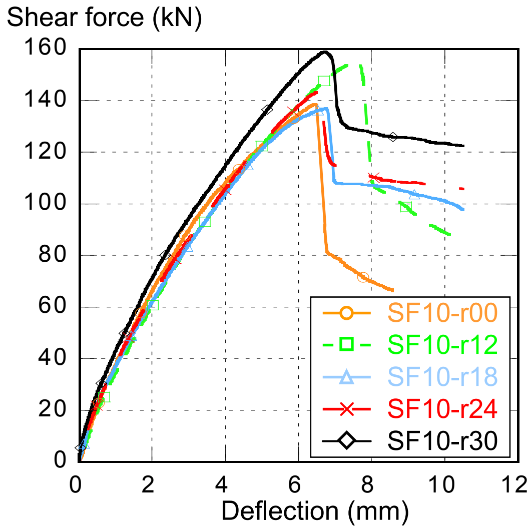

Fig. 4 Shear force-deflection curves

All beams expressed a linear behavior from the initial load to the first flexure crack. The first cracking in flexure appeared at the same load level for all investigated beams and then propagated to the top of specimens with increasing in the shear force.

The diagonal crack was observed around the middle height of specimens when shear force was around 80 kN. This shear force did not significantly change among specimens. Consequently, the increase of r_w did not affect the diagonal cracking strength of RSF beams. The results showed that the appearance of diagonal crack reduced the slope of shear force-deflection curve of RSF beams. After the initiation of diagonal crack, the diagonal crack propagated to supports and the top of specimens. Most of stirrups in investigated beams showed the yielding strain in this stage. However, the propagation of diagonal crack length stopped when the diagonal crack reached the compression zone around 50 mm from the top of specimens. From this step, the rate of increment load was slight and the shear force-deflection curves showed nonlinear behavior. Then, the shear force reached to the peak and the load suddenly dropped due to crushing of concrete in compression zone. The shear

Table 3 Experimental results

Specimen	Concrete properties			Diagonal crack				Experimental results				Calculation		Comparisons		
	SF (%)	r_w (%)	f'_c (N/mm^2)	u^{*1} (mm)	L^{*2} (mm)	$\beta_{avg}{}^{*3}$ (°)	$\theta_{avg}{}^{*4}$ (°)	V_{exp} (kN)	V_c (kN)	V_s (kN)	V_{fexp} (kN)	V_{fcal} (kN)	V_{fpre} (kN)	κ_{exp}	V_{fexp} $/V_{fcal}$	V_{fexp} $/V_{fpre}$
SF10-r00	1.0	0.00	64.9	1.54	539	27.9	66.9	141.1	59.4	0.0	81.7	73.5	79.2	1.38	1.11	1.03
SF10-r12	1.0	0.12	53.0	1.12	493	33.4	62.5	155.5	55.5	12.9	87.2	83.5	77.0	1.57	1.04	1.13
SF10-r18	1.0	0.18	46.6	1.10	422	35.1	62.4	136.8	53.2	19.3	64.4	63.4	76.5	1.21	1.01	0.84
SF10-r24	1.0	0.24	48.3	0.94	439	34.0	63.1	143.1	53.8	26.9	62.4	71.6	75.4	1.16	0.87	0.83
SF10-r30	1.0	0.30	55.3	0.67	387	34.0	63.3	158.8	56.3	32.1	70.3	72.6	73.7	1.25	0.97	0.95

*1: average crack surface displacement at the peak, *2: total crack length at the peak, *3: average angle of diagonal crack at the peak, *4: average angle of principal tensile strain angle at the peak

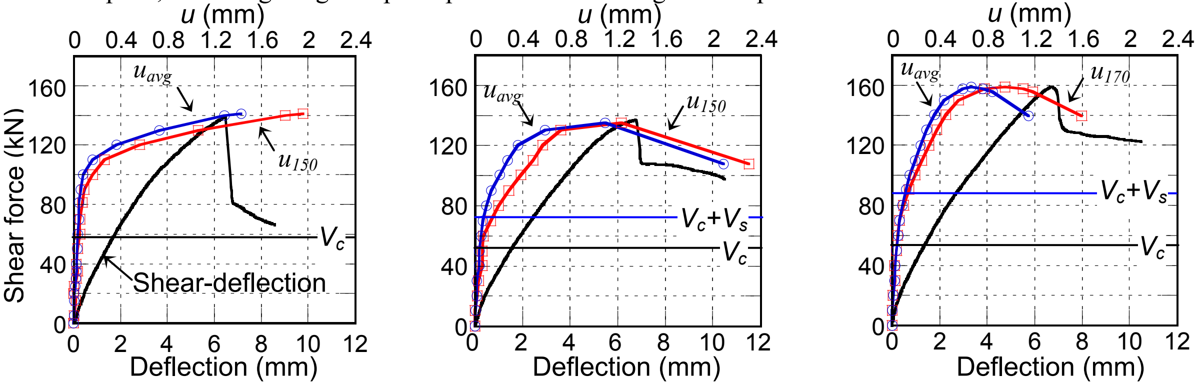

(a) SF10-r00 (b) SF10-r18 (c) SF10-r30

Fig. 5 Development of crack surface displacement and deflection

failure happened in all beams. With the increase in r_w, the reduction of shear force just after the peak became smaller because of the resistance by stirrups.

3.4 Development of diagonal crack

Only one critical diagonal crack was remarkable in each specimen. This paper focused on the tensile force along this diagonal crack. The crack surface displacement and the length of diagonal crack were discussed.

(1) Crack surface displacement (u)

After the appearance of diagonal crack, u increased with the increase in shear force as shown in Fig. 5. The crack surface displacement at 150 mm and 170 mm from the bottom of specimens (u_{150}, u_{170}) are plotted in the top horizontal axis together with shear force-deflection curve. In addition, Fig. 5 shows the average value of crack surface displacement (u_{avg}) of diagonal crack except for the compression zone and concrete cover. The compression zone was the height of specimens between 0 mm to 50 mm from the top fiber according to the location of neutral axis. The neutral axis was calculated from the displacements of targets obtained through the image analysis. V_c and V_c+V_s calculated by Eqs. 5 and 6 are presented by horizontal lines. From Fig. 5, u_{150} and u_{170} showed the similar shape of curves with u_{avg}. After the generation of diagonal crack, the values of u increased linearly with the increase in shear force. Then, u increased suddenly before the peak load. This increase in u corresponded to the shear force when the shear force-deflection curve began to show nonlinear behavior. This implied that the sudden increment of u would relate to the peak and lead the failure of RSF beams. The sudden growth of crack before the load reached the peak, however, tended to decrease when the stirrup ratio increased. These results implied that stirrups could prevent the growth of diagonal crack.

Figure 6 shows the crack surface displacement along the height of specimens at the maximum shear force of three specimens. Unlike the flexure crack, the diagonal crack surface displacement was larger at around the middle height of specimens compared with the crack surface displacement at the top and bottom of specimens. This was because there was compression zone at top of specimens or restraint by longitudinal reinforcing bars. In addition, this figure shows that u decreased with the increase in r_w as listed in Table 3. These results confirmed that the addition of stirrups to RSF beams reduced the crack surface displacement of diagonal crack.

Since the crack surface displacement of diagonal crack at the peak load is a key to investigate the shear carried by steel fibers in this paper, it is important to measure u at the maximum load. Thus, some pictures were taken near the peak load with short time interval in order to capture the behavior at the peak exactly. Moreover, the picture at the maximum load was compared with other pictures around the peak to confirm that the difference between these pictures was insignificant.

(2) Crack length (L)

The crack length (L) was length of the diagonal crack from 50 mm from top fiber to the location of longitudinal reinforcements. The experimental results showed that, with the increase in r_w, L decreased as summarized in Table 3.

3.5 Shear carried by steel fibers

(1) Calculation method of shear carried by steel fibers

In order to investigate the shear carried by steel fibers (V_{fcal}), specimens were considered as 15 layers

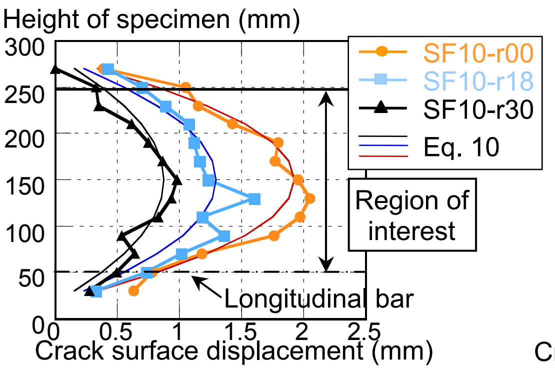

Fig. 6 Crack surface displacement distribution

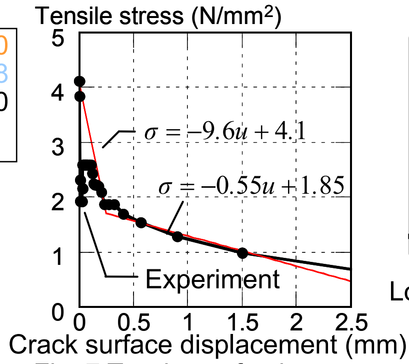

Fig. 7 Tension softening curve

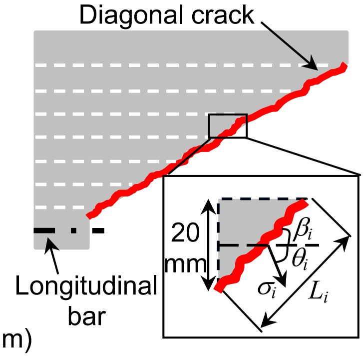

Fig. 9 Free body diagram

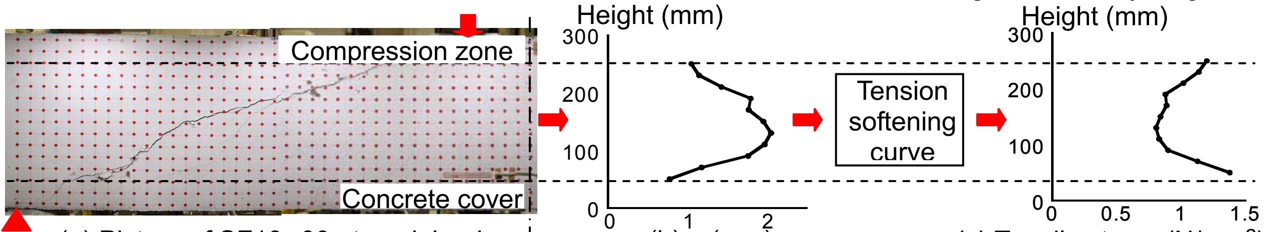

(a) Picture of SF10-r00 at peak load (b) u (mm) (c) Tensile stress (N/mm²)

Fig. 8 Calculation procedures of shear carried by steel fibers based on tension softening curve

with a height of 20 mm. Crack surface displacement (u_i), length (L_i), angle of principal tensile strain (θ_i), and angle of a diagonal crack of each element (β_i) were investigated.

The tension softening curve of concrete with SF=1.0% is presented in Fig. 7. Tension softening curve was calculated through "tension softening curve poly-linear approximation" according to JCI [6]. Splitting tensile strength of concrete was 4.1 N/mm². The fracture energy (G_F) was 3262 N/m. The curve was used for converting u_i to tensile stress (σ_i) transferring along the diagonal crack. The calculation procedures of shear carried by steel fibers based on tension softening curve are shown in Fig. 8.

By considering the force acting at a diagonal crack in a RSF beam due to the effect of steel fibers (Fig. 9), the tensile force along the diagonal crack of each element can be obtained by multiplying σ_i with the area of crack surface normal to the direction of σ_i. The vertical component of this force with the consideration of θ_i was the shear carried by steel fibers. According to Fig. 9, the force along the diagonal crack was obtained except for the compression zone and concrete cover. The region of interest is shown in Fig. 6. The shear carried by steel fibers (V_{fcal}) can be expressed as follows;

$$V_{fcal} = \sum_{i=1}^{11}\left(\sigma_i \cdot b_w \cdot L_i \cdot \cos(\theta_i + \beta_i - 90) \cdot \sin\theta_i\right) \quad (9)$$

According to Eq. 9, V_{fcal} increases with the increment of L_i. On the other hand, V_{fcal} decreases with the increment of u_i. However, the experimental results showed that L_i and u_i decreased with the increase in r_w. As a result, V_{fcal} in each specimen was different even the volume fraction of steel fibers was identical.

(2) Comparison of calculated and experimental values of shear carried by steel fibers

The results of calculated shear carried by steel fibers (V_{fcal}) using Eq. 9 and the experimental value (V_{fexp}) using Eq. 7 are shown in Table 3. Figure 10 shows the variation of V_{fexp}/V_{fcal} with respect to r_w.

The comparison demonstrated that V_{fcal} provided good agreement with V_{fexp}. These findings implied that the shear carried by steel fibers could be evaluated by using the tension softening curve. Consequently, this hypothesis is effective for predicting the shear carried by steel fibers.

3.6 Predictive equation for shear carried by steel fibers (V_{fpre})

For all specimens, the parabolic relation between u_i and h_i in Eq. 10 would be applied as shown in Fig. 6. In this paper, the parabolic equation of SF10-r18 was used as a control equation. Then, u_i as functions of r_w and h_i was formulated based on the relation between control equation and r_w. The equation of u_i along the height of diagonal crack (h_i) was proposed as Eq. 10. The value of u_i calculated from the equation was presented in Fig. 6.

$$u_i = a \cdot \left(-6 \times 10^{-5} h_i^2 + 0.017 h_i + 0.13\right) \quad (10)$$

where, a: effect of r_w on u_i (a = 1.3-2r_w), h_i: height from bottom fiber of specimens.

In order to convert u to σ, the equation of tension softening curve was needed. A bilinear stress-separation curve was used as presented in Eqs. 12 and 13 as shown in Fig.7.

From the experimental results of five RSF beams with different r_w, the tendency between L_i and h_i could not be expressed. Hence, the total length of diagonal crack (L) in the region of interest was used for expressing the relationship between L and r_w. From the reason that L decreased with the increase in r_w (Fig. 11), Eq. 14 was formulated. Figure 11 shows the measured and predictive values of L.

With regard to the angle of principal tensile

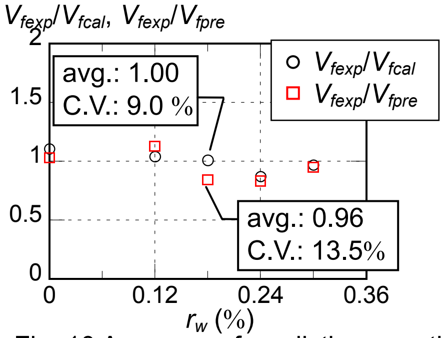

Fig. 10 Accuracy of predictive equation

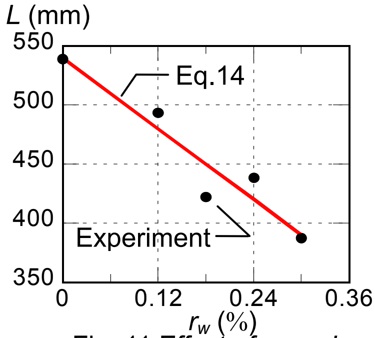

Fig. 11 Effect of r_w on L

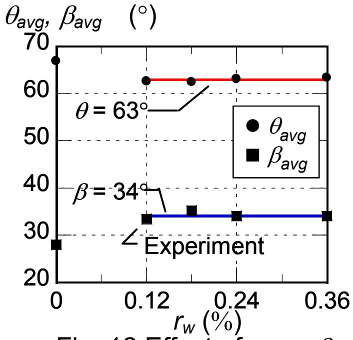

Fig. 12 Effect of r_w on β

strain (θ_i), no tendency was observed in the distribution of θ_i along the height of specimens. For this reason, the average value of the angle of principal tensile strain (θ_{avg}) was used for investigating the relationship between θ_{avg} and r_w. The values of θ_{avg} are listed in Table 3 and shown in Fig. 12. The results show that θ_{avg} was constant (63 degrees) in the specimens with stirrups. However, θ_{avg} was 67 degrees in the specimen without stirrup.

As same with θ_i, the tendency of β_i with respect to h_i has not been observed. The average value of angle of diagonal crack (β_{avg}) was 34 degrees in the specimens with stirrups and β_{avg} was 28 degrees in case of no stirrup as shown in Fig. 12.

The shear carried by steel fibers of RSF beams with stirrups can be predicted by Eq. 11.

$$V_{fpre} = \sigma \cdot b_w \cdot L \cdot \cos(\theta + \beta - 90) \cdot \sin\theta \qquad (11)$$

where,

V_{fpre} = predictive shear carried by steel fibers (kN)

σ = tensile stress along diagonal crack (N/mm^2)

= $-9.6u + 4.1$ for $u < 0.25$ mm (12)

= $-0.55u + 1.85$ for $u \geq 0.25$ mm (13)

b_w = web thickness (mm)

L = crack length of region of interest (m)

= $0.54 + 0.5r_w$ (14)

θ = angle of principal tensile strain (°)

β = angle of diagonal crack (°)

It is noted that u used for calculating V_{fpre} is the average value of all u_i in the region of interest.

The predicted value of shear carried by steel fibers is listed in Table 3. Figure 10 shows the variation of V_{fexp}/V_{fpre} with respect to r_w. Although, V_{fpre} provided a less agreement with V_{fexp} than V_{fcal}, V_{fpre} can predict the shear carried by steel fibers. Therefore, the shear carried by steel fibers will be estimated by this proposed equation. These findings confirmed that the shear carried by steel fibers can be evaluated by using the tension softening curve. By considering others factors affecting on shear carried by steel fibers, the equation will cover widely and give better accuracy.

4. CONCLUSIONS

(1) It is not necessary that the shear capacity of RSF beams will increase with the increase in stirrup ratio because the value of shear carried by steel fibers in each specimen was different.

(2) The crack surface displacement of diagonal crack increased drastically before the peak load corresponded to shear force when the shear force-deflection curve showed nonlinear behavior.

(3) The crack surface displacement of diagonal crack around the middle height of specimens was larger than those at top and bottom fiber of specimens.

(4) With the increase in stirrup ratio, the crack surface displacement and the length of diagonal crack of RSF beams decreased.

(5) The shear carried by steel fibers calculated using the tension softening curve corresponded to the experimental value.

(6) Based on experimental results, the equation for predicting shear carried by steel fibers for RSF beams with different stirrup ratio was suggested. The shear carried by steel fibers can be estimated by this equation.

ACKNOWLEDGEMENT

The authors acknowledge the supports of Grant-in-Aid for Scientific Research (A: No.19206050) from JSPS and the foundation "Hattori-Hokokai".

REFERENCES

[1] JSCE, "Standard Specifications for Concrete Structures-2002, Structural Performance Verification", JSCE Guidelines for Concrete, No.3, pp.76-83, 2005

[2] Sharma, A. K., "Shear Strength of Steel Fiber Reinforced Concrete Beams", ACI Journal, Vol. 83, No. 4, pp.624-628, Jul.-Aug. 1986

[3] JSCE, "Guidelines of Design for RSF Piers", Concrete Library 97, p.15, 1999 (in Japanese)

[4] Watanabe, K. et al., "Shear Reinforcement for RC Linear Members by a Combination of Steel Fibers and Shear Reinforcing Bars", Journal of Materials, Concrete Structures and Pavements, Division E, JSCE, Vol. 65, pp.322-331, Jul. 2009 (in Japanese)

[5] Higashi, H., Watanabe, K., and Niwa, J., "Image Analysis for Failure Mode of RC Beams with Fractured Longitudinal Reinforcement", Proceedings of the JCI, Vol.31, No.2, pp.727-732, Jul. 2009 (in Japanese)

[6] JCI, "Method of Test for Fracture Energy of Concrete by Use of Notched Beams", Japan Concrete Institute Standard, 2003